EFFECT OF ASPECT RATIO AND BIFURCATION ANGLE ON SINGLE PHASE FLOW THROUGH BRANCHED STRUCTURE MICROCHANNEL

A Thesis by

Pavan Vellore Kumaraswamy

Bachelor of Engineering, Sir M Visvesvaraya Institute of Technology, 2010

Submitted to the Department of Mechanical Engineering
and the faculty of the Graduate School of
Wichita State University
in partial fulfillment of
the requirements for the degree of
Master of Science

December 2017

EFFECT OF ASPECT RATIO AND BIFURCATION ANGLE ON SINGLE PHASE FLOW THROUGH BRANCHED STRUCTURE MICROCHANNEL

The following faculty members have examined the final copy of this thesis for form and content, and recommend that it be accepted in partial fulfillment of the requirement for the degree of Master of Science with a major in Mechanical Engineering.

_____

T. S. Ravigururajan, Committee Chair

_____

Krishna Krishnan, Committee Member

_____

Brian Driessen, Committee Member

ACKNOWLEDGEMENT

My sincere thanks to my advisor and graduate coordinator Dr. T. S. Ravigururajan for providing guidance and endless support throughout my master's degree at Wichita State University. I also thank my committee members Dr. Krishna Krishnan and Dr. Brian Driessen for taking time out of their busy schedule to evaluate my work and providing their valuable suggestions.

I would like to extend my gratitude to my family and friends for their unconditional love and support. I am very fortunate to have such great minds and good-hearted people around me, providing motivation and zeal to achieve my goals.

ABSTRACT

The introduction of microchannel heat exchangers (MCHE) has revolutionized the cooling technology which has led to the miniaturization of devices. MCHEs are highly preferred in many applications because of their characteristic large heat transfer area to unit volume leading to higher efficiency compared to conventional heat exchangers. Due to their compactness, they are mainly used in electronic cooling; in recent times, their application is extended to the medical field for cooling scanning equipment. However, the small channel size increases pressure drop. Present study focuses on optimizing the performance of the MCHEs by carrying out single phase flow analysis of lung bronchial like branched structure in ANSYS (Fluent) with different aspect ratios (AR) between 0.5, 1.0, 1.5 and 2.0 at the inlet, and at different bifurcation angles of 30, 45 and 60 and 70 degrees.

Symmetric geometry containing four bifurcation levels were designed. A number of geometries were created for varying bifurcation angle and varying aspect ratio. Simulations were carried out for steady state and laminar flow conditions. Results so far show that pressure drop decreased with increase in AR and achieved better uniformity in temperature throughout the channel length for higher AR.

TABLE OF CONTENTS

LIST OF TABLES

Table Page

LIST OF FIGURES

LIST OF FIGURES (continued)

Figure Page

NOMENCLATURE

H – Height of the channel (m)

W – Width of the channel (m)

L – Length of the channel (m)

D – Diameter of the channel (m)

D_h – Hydraulic diameter (m) [same as diameter for circular channels]

Le – Entrance length (m)

AR – Aspect Ratio (H/W)

Re – Reynolds number

A – Cross-sectional area of channel (m^2)

P – Wetted perimeter (m)

Q – Volume flow rate (m^3/s)

P – Density of the working fluid (m^3/kg)

μ – Absolute viscosity (kg/m-s)

CHAPTER 1

INTRODUCTION

Heat exchangers are devices that allow thermal energy transfer between two or more fluids at different temperatures. They are used in wide range of applications; these include food and chemical industries, electronic cooling and packaging, air conditioning (HVAC) and refrigeration industries, Medical equipment, waste heat recovery systems, manufacturing and process industries, and space applications. Heat exchangers are mainly classified as Recuperators and Regenerators; further classification is done based on heat transfer process (conduction, convection, and radiation), flow arrangement (parallel, counter or cross-flow), heat transfer mechanism (single-phase and two-phase), geometry, etc.

In the past two decades, Microchannel Heat Exchangers (MCHE) has gained a lot of interest among researchers' due to its high heat transfer efficiency compared to that of conventional heat exchangers. MCHEs are distinguished from conventional HE by the characteristic flow diameter of the channel, which corresponds to the hydraulic diameter of the conduit in case of rectangular channels, $D_h \leq 1000\mu m$ [2].

Most of the researchers in the field acknowledge the first ever application of microchannel heat sink by Tuckerman and Pease [1] for cooling integrated circuits to have opened the door to a whole new field of research. Since then, numerous investigations on straight channels, cross flow and branched channels (fractal structure) were carried out to determine the fluid flow and heat transfer characteristics in microchannels.

A substantial amount of research has been done on rectangular MCHE both single and array of parallel channels, results of which are discussed in the literature review.

The present study concentrates on fractal structure, the design closely related to nature in the mammalian vascular system or tree branching; known to be highly efficient in transporting blood, oxygen, water, and food. The human lungs are the most efficient heat exchangers known to humanity, therefore heat exchangers with better flow characteristics and heat transfer efficiency can be designed by the knowledge gained from the study.

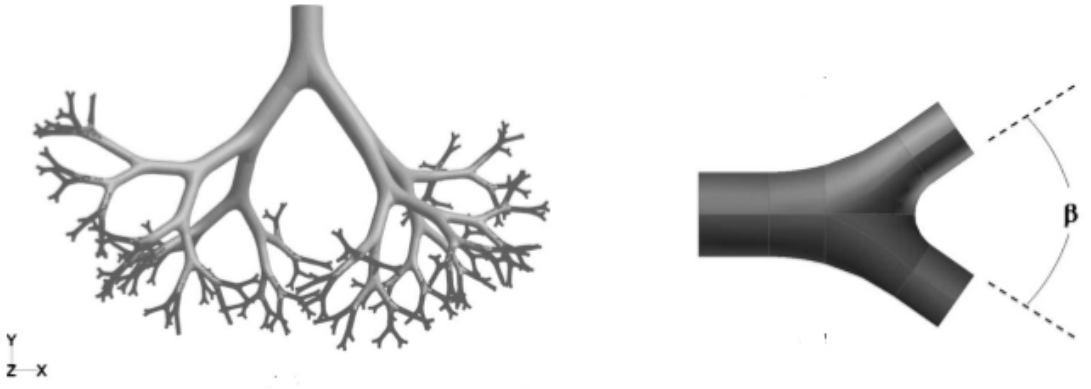

(i) (ii)

Figure 1 (i)Eight-generation model of bronchial region based on Weibel's lung morphology (ii) Parent-daughter branching unit ($\beta = 70^{\circ}$) [3]

A method to study the large-scale regions of the human lung airways by three dimensional Navier-Stokes simulation was proposed by D. Keith Walters et al. Figures 1(i) & 1(ii) [3] shows the eight-generation model of the bronchial region and parent-daughter branching unit developed by Walters based on Weibel's lung morphology.

CHAPTER 2

LITERATURE REVIEW

A three-dimensional model of Lung airflow region developed by Walters et al. was based on the Weibel's lung morphology [4]. The assumptions of Weibel's model was as follows:

- Branching angle (β) was assumed to be 70 degrees and uniform to all branches
- Length to diameter ratio (L/D) = 3
- Parent to daughter diameter ratio (D_p/D_d) = 1.33

These were approximations drawn based on available morphological data. Walter's model extended in three dimensions by rotating the bifurcation plane randomly between angles 0 to 180 degrees. If the branches intersected, then the angle was changed and remodeled at that region. Although this model predicted the pressure drop and mass flow rate within a certain percentage of the simulated results predicted by the fully resolved model, the computational cost reduced by a sizable amount.

A one-dimensional analysis of pressure distribution and channel wall temperature in a fractal-like structure was carried out by Deborah V. Pence [5]. The branching structure was based on the mammalian circulatory system proposed by West et al. [7]. An analogy is assumed to be existing between metabolic and thermal transport processes. The system consisted of various scaling laws to determine the width and length of the structure.

$$\alpha = \frac{d_{k+1}}{d_k} = n^{-1/AC}$$

$$\gamma = \frac{L_{k+1}}{L_k} = n^{-1/D}$$

The depth of the channel and width of the terminal branch were fixed, from which the width of the k^{th} level branches was determined from the $k+1^{th}$ level branch. In this system, the total length of the channel was also fixed and with the help of equation the lower level branching lengths were determined using equations:

$$w_k = \frac{w_{k+1}H}{\beta(w_{k+1} + H) - w_{k+1}}$$

$$L_m = \frac{L_{tot}}{\sum_{i=0}^{m}(1/\gamma^i)}$$

The pressure-drop and maximum wall temperature from the simulation result were compared to straight channel array of similar cross-section area at the terminal branch, flow conditions, etc. and found to be much lower. Although thermal resistance through the fractal channel was higher in comparison with a straight channel for the same convective surface area because of other advantages fractal structure is better than a straight channel for cooling.

A three-dimensional asymmetrical model was developed by Alharbi et al. [8] based on the flow network proposed by Pence. The objective of the study was to determine how close does a one-dimensional analysis predicts the flow properties in fractal structure when compared to the flow analysis carried out by a three-dimensional model. The results show the pressure drop predictions by the one-dimensional model was within 4% of that predicted by the three-dimensional model for straight channels but was approximately 30% for that of fractal structure. And the reason for such large variation in the fractal structure was attributed to local pressure recovery at each bifurcation.

Alharbi et al in yet another study following the same structure and assumptions investigated heat transfer through straight and fractal network [9] using a three-dimensional model approach and compared to the results predicted by the one-dimensional model. Developing flow conditions were assumed following each bifurcation and results indicate this assumption is acceptable, although the thermal boundary does not redevelop at the walls of the channel following each bifurcation. For the same flow rate and applied heat flux, there was large temperature variation along fractal network with a slight increase in pressure drop compared to given geometric and flow conditions in straight channel heat sink. It was recommended that a study be carried out to determine the effect of bifurcation angle and include varying thermophysical properties.

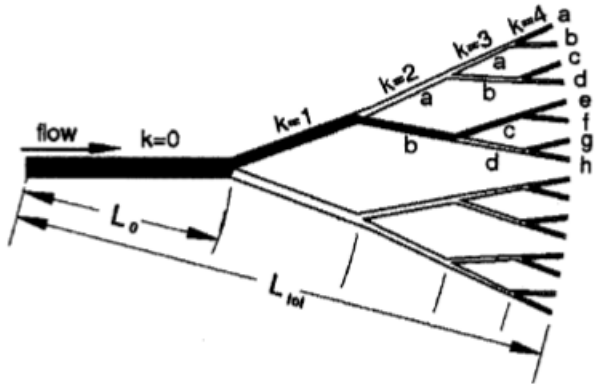

Figure 2. Asymmetric Fractal-like branching network [8]

In yet another study based on the same branching ratios proposed by Pence, Wang et al [10], studied the effect of bifurcation angle in branched structure microchannel network. A symmetric three-dimensional computational model was developed by Wang to predict the fluid flow and heat transfer characteristics through varying bifurcation angle. The results indicated that the flow field and the thermal pattern deteriorates with increase in the bifurcation angle. Even with large bifurcation angle,

the pressure drop in the fractal structure was less than that in the straight channels. The mass flow rates and bulk temperatures varied with each outlet indicating a non-symmetrical flow, though the branching was symmetrical.

The flow-through fractal structure was discussed so far, although present study focuses on the fractal structure it is equally important to discuss straight channels of different cross-section as after each bifurcation these channels represent a rectangular straight channel.

A comparative analysis of studies on heat transfer and fluid flow in microchannel by Sobhan and Garimella [12] is a review of experimental work carried out by various researchers prior to 2000. This review article contains results of investigations under diverse topics such as Microchannel concept and early work, Single-phase (liquid) experiments and model optimization studies, Gas flow, Boiling in microchannel, Design, and testing, etc.

Studies by Tuckerman & Pease demonstrated the use of microchannels for high convective heat transfer in cooling integrated circuits (790 W/cm^2) for a temperature difference of 71˚C between the substrate and the coolant.

Wu & Little [13] measured friction factor in microchannel (D_h = 55-76μm) and compared the results with that of commercial channels. Observed 3-5 times larger value of friction factor for glass channels compared to smooth-pipe predictions and occurrence of flow transition at Re ≈ 400. Also formulated correlations for friction factor and Nusselt number for a wide range of Reynold's number.

It is concluded that the flow and heat transfer characteristics of microchannel and that of conventional heat exchangers are different but the reason for such variation was not presented in the literature studies carried out by the authors. It is predicted

that the variations may be due to the entrance and exit effects, differences in surface roughness of the channels, difference in channel dimensions, errors in instrumentation, measurement location, and nature of flow and thermal boundary conditions.

“Heat transfer in microchannels – 2012 Status and Research needs” a review publication by Kandlikar et al [14], discusses the research on the topic in the period 2000-2012. The author mentions this period as a resurgence in the research on MCHE as a vast number of publications were produced which provided greater knowledge into the subject.

CHAPTER 3

METHODOLOGY

3.1 Method of Approach

Initial geometry model was developed based on Weibel's morphology from which hydraulic diameter and channel length were calculated. Hydraulic diameter for the $K+1^{th}$ branch was calculated based on dimensions of K^{th} branch by the relation $D_k/D_{k+1} = 1.33$ and the length of a branch is calculated by the relation $L/D_h = 3$. Four different aspect ratios (AR = H/W) - 0.5, 1, 1.5 and 2 were considered along with four different angles of bifurcation i.e., 30˚, 45˚, 60˚ and 70˚. The aspect ratio mentioned above corresponds to channel K = 0, from inlet up to the first bifurcation as shown in figure 3.1.

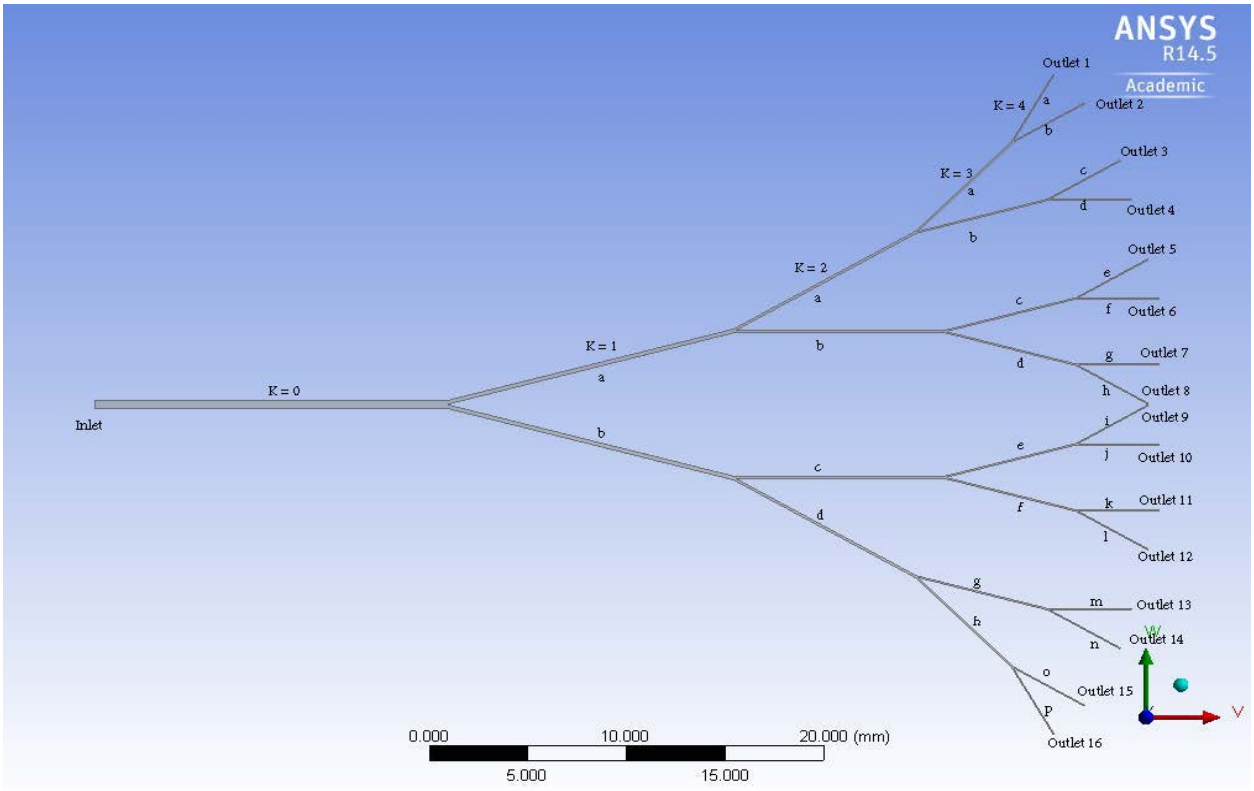

Figure 3.1. Top view of the branching network showing branching levels and labels.

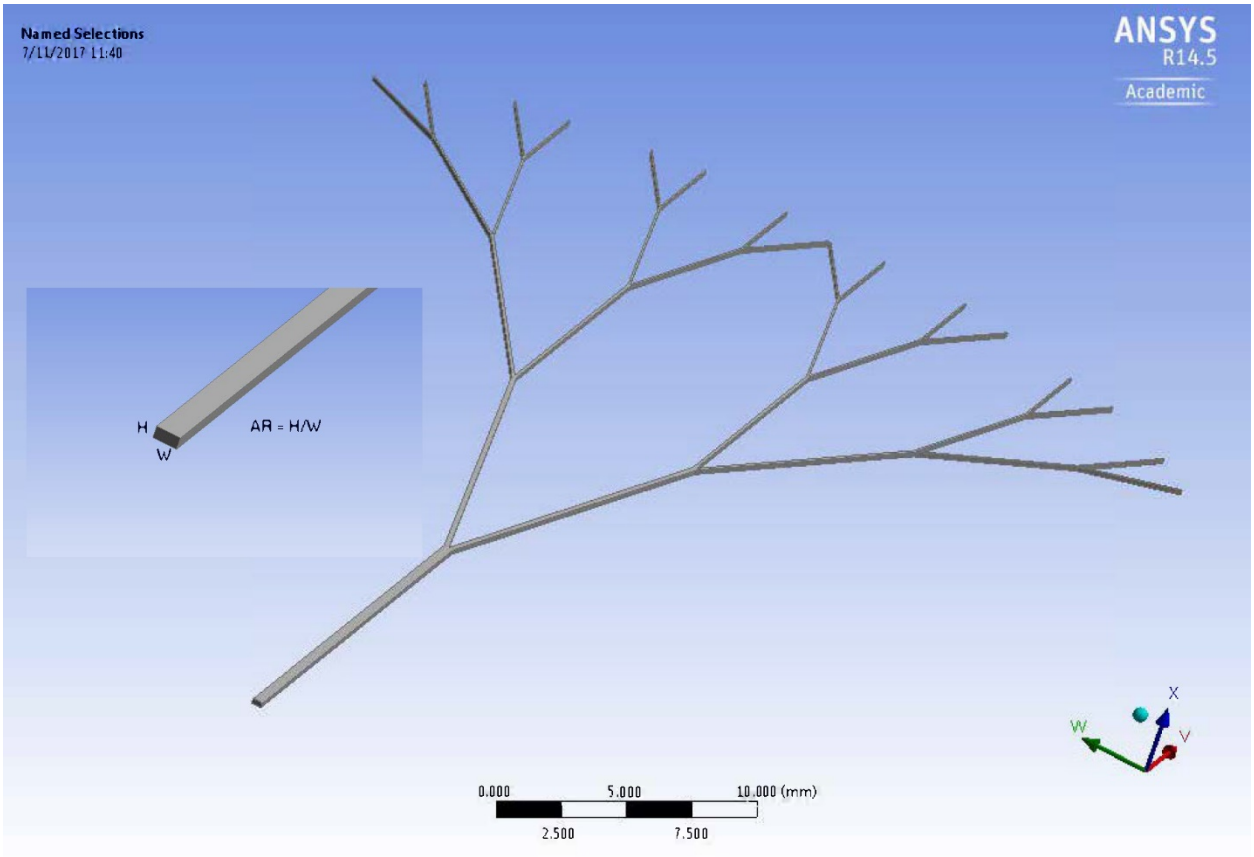

Figure 3.2. ISO view of the branching network

The aspect ratio of 1.5 was fixed at channel K = 0, the pressure drop, velocity and temperature variation through the channel were simulated for varying bifurcation angle (30, 45, 60 & 70 degrees). After post-processing, bifurcation angle with least pressure drop i.e., flow with least resistance was determined.

For next set of simulations, the aspect ratio is changed at the inlet from 0.5 to 2.0 and four different models are designed by fixing the bifurcation angle with least resistance to flow (information from the previous set of simulations). Although variation in AR applied only at the inlet, AR increases due to decrease in width of the channel (height of the channel kept constant). The results of the simulations to be discussed later in section 5.

Another geometry model was developed to focus on fully developed flow. The velocity was fixed based on the flow rate of air in human lungs [3]. From which Reynold's number and entrance lengths were calculated. In internal flow, speed of the fluid close to walls reduces to zero due to wall friction. The speed of fluid flowing at the centerline (inviscid) must increase to follow mass conservation law for incompressible flow. Hence the velocity profile changes from the entrance to a certain region in the pipe. At a sufficient distance from the entrance, the developing boundary layer at the wall reaches the centerline and flow becomes totally viscous and the profile no longer changes. The regions are visually described in figure 3.3 and the entrance length (Le) calculation through equation given below.

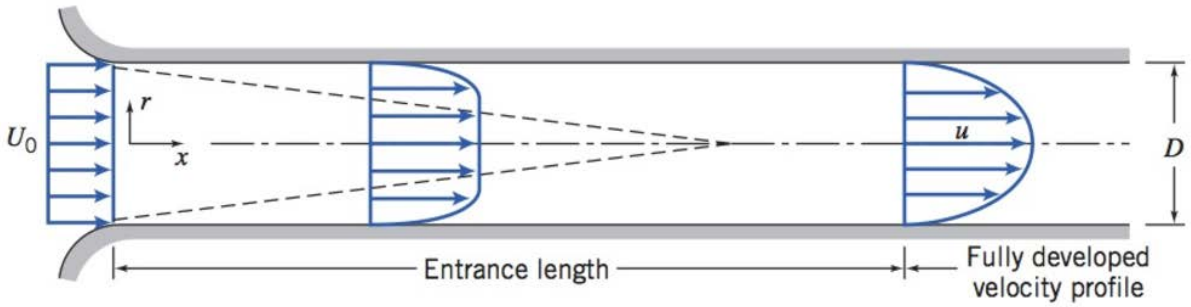

Figure 3.3. Flow in the entrance region of a pipe [28]

$$\frac{L_e}{D_h} = 0.06 * Re$$

The channel lengths were set to five and ten times the entrance length to give sufficient length for the fluid to flow in the developed region to determine the pressure drop and heat transfer characteristics through the channel. Pressure drop and temperature rise were determined across the channels. The gauge pressure at the outlet was set to zero, therefore the calculated pressure at the inlet would be the pressure drop across the length of the channels.

3.2 Geometry:

Hydraulic diameter (D_h) changes with change in aspect ratio, entrance length has a direct impact with a change in hydraulic diameter as shown in equations. To estimate inlet velocity the volume flow rate of 10.42 cm^3/s for an inhalation rate of 167cm^3/s for a D_h value of 0.57cm was considered [3]. The values were scaled according to the channel dimensions considered in the present study with respect to D_h.

$$D_h = \frac{4A}{2P} = \frac{4 * Cross\ section\ area}{Wetted\ perimeter}$$

In rectangular channels, the cross-sectional area does not change from inlet to outlet. As it remains constant determining the flow characteristics due to varying aspect ratio could be estimated by simple steps. In contrast, in fractal structure the cross-sectional area reduces after each bifurcation due to reducing width of the channel. The aspect ratio mentioned earlier in relation to fractal structure corresponds to the channel K=0 (the channel from the inlet to 1st bifurcation). The width of the inlet channel is fixed for all the aspect ratios. That is, the aspect ratio is varied by varying the height of the inlet channel (K=0). Table 1 contains the channel dimensions and a better understanding of the geometry could be achieved by observing the values in the table.

Table 1

Aspect ratio and dimensions of inlet channel (K=0)

Channel H (m)	Channel W (m)	AR
0.000200	0.000400	0.5
0.000400	0.000400	1.0
0.000600	0.000400	1.5
0.000800	0.000400	2.0

Table 2

Channel dimensions from inlet to exit after each bifurcation and their aspect ratios for inlet channel aspect ratio = 2.0

Channel H (m)	Channel W (m)	AR
0.000800	0.000400	2.0
0.000800	0.000268	3.0
0.000800	0.000186	4.3
0.000800	0.000132	6.1
0.000800	0.000095	8.4

Inlet velocity and Reynold's number determined from below equations with other geometry parameters tabulated and presented in Tables 3, 4, 5 and 6 for varying inlet channel AR.

$$v = \frac{Q}{A}$$

$$Re = \frac{\rho * v * D_h}{\mu}$$

Table 3

Channel dimensions and flow conditions for Inlet channel AR 0.5

Channel H (m)	Channel W (m)	D_h (m)	Q (m^3/s)	V (m/s)	Re	AR	Le (m)	Le*10 (m)
0.000200	0.000400	0.000267	0.487485	6.09	111	0.5	0.001780	0.017799
0.000200	0.000201	0.000201	0.366530	9.12	125	1.0	0.001506	0.015055
0.000200	0.000121	0.000151	0.275587	11.39	118	1.7	0.001063	0.010633
0.000200	0.000079	0.000113	0.207208	13.10	102	2.5	0.000691	0.006913
0.000200	0.000054	0.000085	0.155796	14.39	84	3.7	0.000429	0.004292

Table 4

Channel dimensions and flow conditions for Inlet channel AR 1.0

Channel H (m)	Channel W (m)	D_h (m)	Q (m^3/s)	V (m/s)	Re	AR	Le (m)	Le*10 (m)
0.000400	0.000400	0.000400	0.731228	4.57	125	1.0	0.003004	0.030035
0.000400	0.000241	0.000301	0.549796	5.70	117	1.7	0.002119	0.021193
0.000400	0.000158	0.000226	0.413380	6.56	102	2.5	0.001377	0.013771
0.000400	0.000108	0.000170	0.310812	7.20	84	3.7	0.000855	0.008547
0.000400	0.000076	0.000128	0.233693	7.68	67	5.3	0.000516	0.005155

Table 5

Channel dimensions and flow conditions for Inlet channel AR 1.5

Channel H (m)	Channel W (m)	D_h (m)	Q (m^3/s)	V (m/s)	Re	AR	Le (m)	Le*10 (m)
0.000600	0.000400	0.000480	0.877474	3.66	120	1.5	0.003460	0.034601
0.000600	0.000258	0.000361	0.659755	4.26	105	2.3	0.002280	0.022796
0.000600	0.000175	0.000271	0.496056	4.72	88	3.4	0.001426	0.014263
0.000600	0.000123	0.000204	0.372975	5.06	71	4.9	0.000865	0.008648
0.000600	0.000088	0.000153	0.280432	5.31	56	6.8	0.000514	0.005137

Table 6

Channel dimensions and flow conditions for Inlet channel AR 2.0

Channel H (m)	Channel W (m)	D_h (m)	Q (m^3/s)	V (m/s)	Re	AR	Le (m)	Le*10 (m)
0.000800	0.000400	0.000533	0.974971	3.05	111	2.0	0.003560	0.035597
0.000800	0.000268	0.000401	0.733061	3.42	94	3.0	0.002262	0.022621
0.000800	0.000186	0.000302	0.551173	3.71	77	4.3	0.001385	0.013849
0.000800	0.000132	0.000227	0.414416	3.92	61	6.1	0.000828	0.008280
0.000800	0.000095	0.000170	0.311591	4.08	48	8.4	0.000487	0.004873

CHAPTER 4

ANSYS FLUENT SOLVER

ANSYS Fluent workbench version 14.5 was used to conduct the computational analysis. Preprocessing, Setup (initial and boundary conditions) and Postprocessing were all carried out in ‘Fluid flow (Fluent)’ analysis tool of the software. Fluid flow (Fluent) consists of various component systems namely Geometry (DesignModeler), Mesh (Meshing), Setup (Fluent), Solution, CFD-Post required to calculate, display and/or plot the solution in the form of graphs, tables, etc.

4.1 Preprocessing

4.1.1. Geometry Modelling: A three-dimensional model of the branched structure microchannel was developed in ANSYS DesignModeler. The details of the geometry were as discussed in section 3. Various sections of the geometry were labeled under ‘Named Selection’ to define the boundary of the geometry that included inlet, outlet, side walls, fluid flow region, etc. Initial and boundary conditions were applied to these boundaries to determine the solution.

4.1.2. Mesh generation: The developed geometry is imported into ‘Meshing’ where the geometry was discretized into smaller elements. The element size was set to coarse, fine and superfine to check for orthogonal quality and aspect ratio. The orthogonal quality value ranges from 0 to 1 and for a superior quality mesh the value must be close to 1. The accuracy of the results depend on quality of the mesh; finer the mesh, longer the computational time taken to solve the problem. Hence, grid convergence method was used to estimate the error in the results for various mesh

sizes and an appropriate size was selected based on the study to limit the mesh size and the accuracy of the solution. Mesh sizing and selection is discussed further in Section 4.2.

4.2 Mesh sizing and selection

Mesh generation is one of the important tasks when performing computational analysis. FLUENT software has an inbuilt mesh tool that can auto-generate coarse, medium and fine mesh as per selection. The generated mesh must be checked for its quality; necessary mesh sizing and refinement can be implemented in order to improve the quality to achieve best results.

A comparison of pressure drop due to different mesh sizes are as shown in Figure 4.1. The software generated fine mesh had a value of 29µm, all other values of mesh sizes were manually entered to determine the appropriate mesh size.

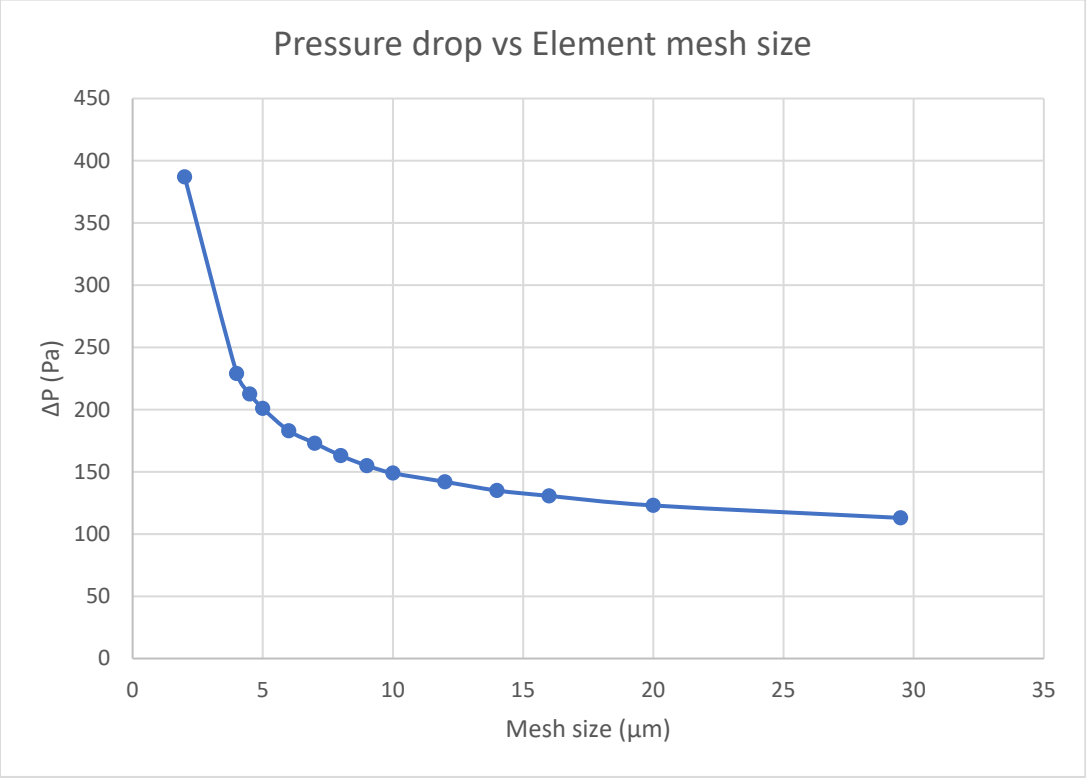

Figure 4.1. Pressure drop versus Mesh size

Pressure drop increases linearly with decrease in mesh size till 10-micron, a further decrease in mesh size leads to higher pressure drop values. Therefore 10-micron mesh size was selected for further simulation studies. Every time mesh quality check was checked to confirm the suitability of 10-micron mesh size for the geometrical dimensions used.

Selecting an appropriate mesh size is essential to reduce the computation time; too fine a mesh leads to large computation time and a coarse mesh leads to an inaccurate solution. The visual appearance of different mesh sizes as shown in Figures 4.2 and 4.3.

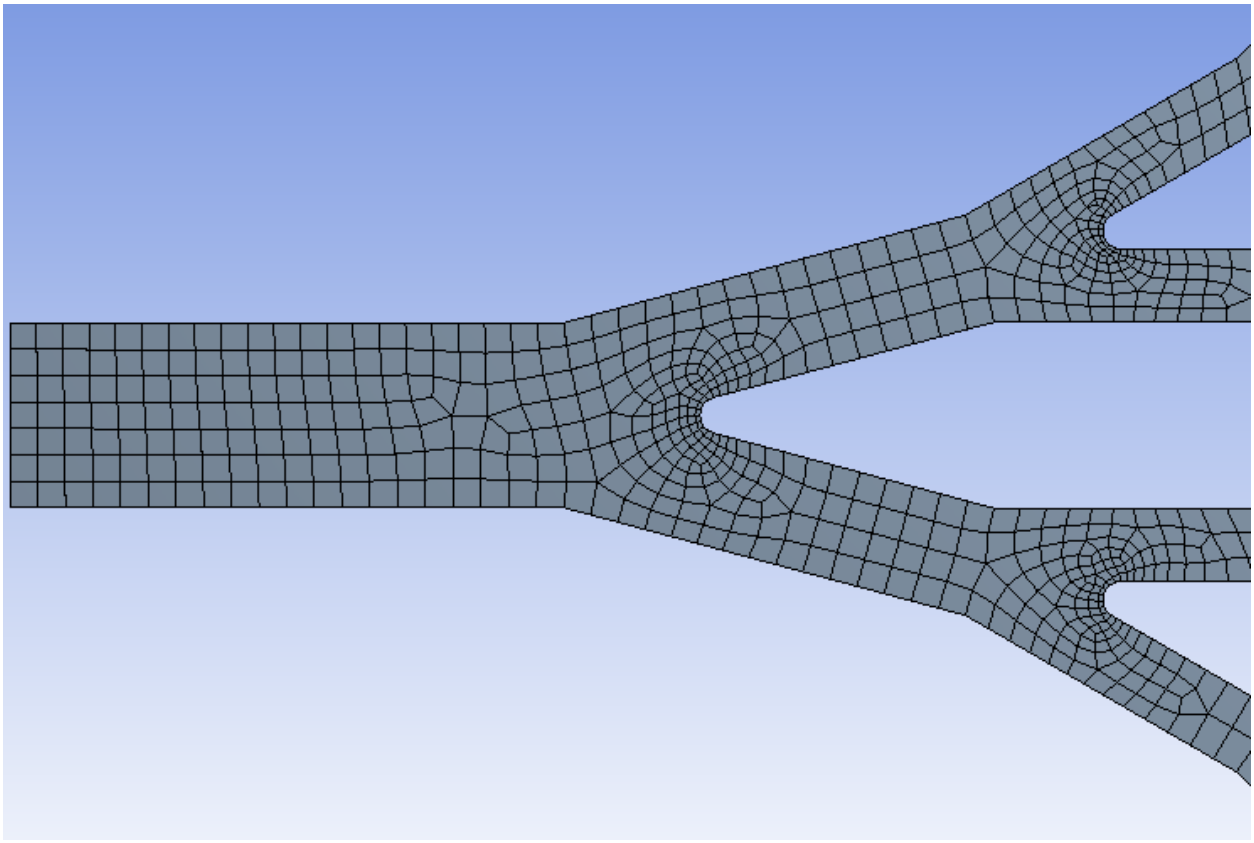

Figure 4.2. Fine mesh generated by FLUENT mesh tool.

As seen from Figure 4.3 with user-defined mesh size, much refined and structured mesh could be generated. The range of aspect ratio of the mesh element is another parameter to determine the quality of the mesh. With a 10-micron mesh size, an aspect ratio of less than 5 was achieved for 95% of the generated mesh elements, and an orthogonal quality of 0.7 achieved overall. In terms of mesh quality, these are really good numbers according to ANSYS Fluent theory guide.[38]

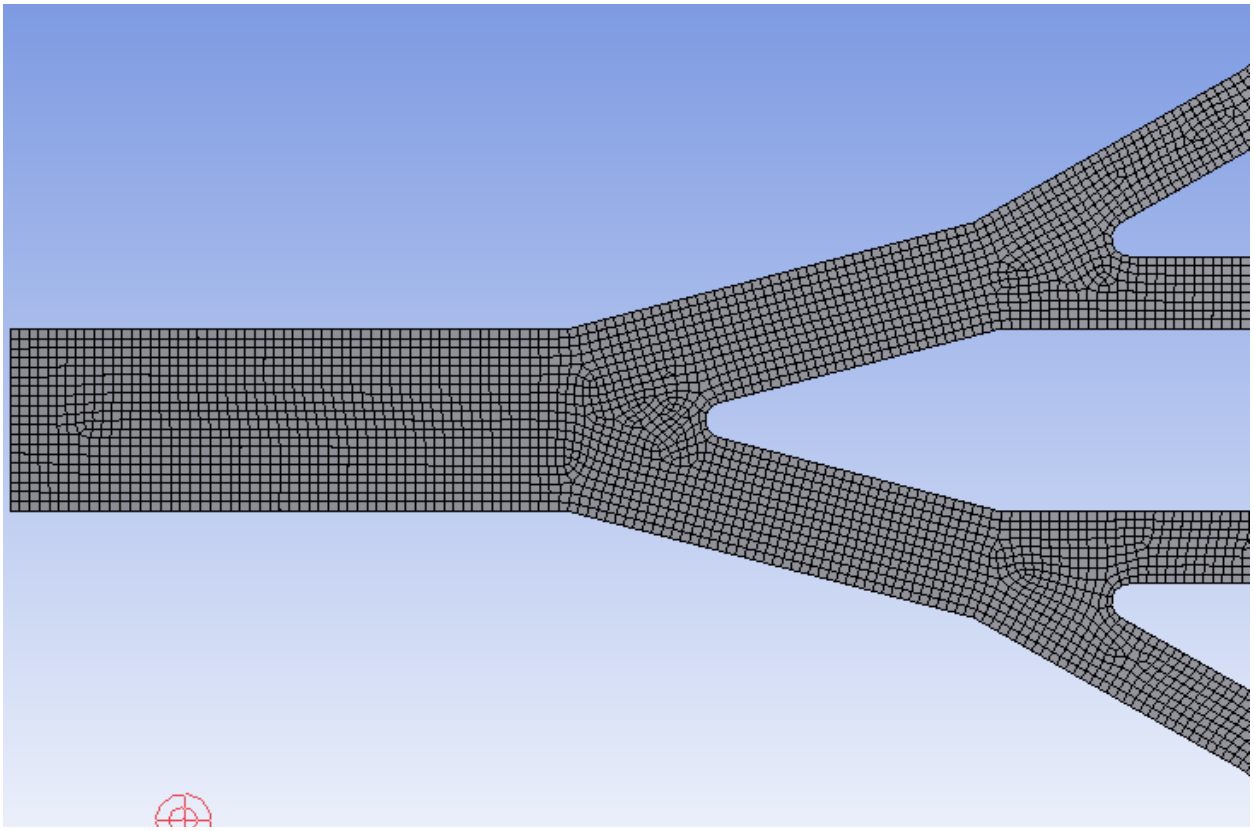

Figure 4.3. User-defined mesh size (10 μm)

4.3 Setup and Post Processing

In this section, the discretized geometry was imported into Fluent, the software evaluated and displayed the total number of nodes, elements of the entire geometry as well as the details at each face of the geometry. Also, a final mesh quality check and report were conducted before starting the simulations. Several parameters were set to run the simulations -

- Pressure-Based, Steady-state solver
- Energy and viscous laminar flow model checked
- Working fluid and wall material properties were fixed by selecting air and aluminum from the software database. The software also allows user-defined properties by directly entering the values.
- Boundary conditions were applied to the fluid and the walls of the channel. Velocity inlet method was set as the flow rate of the fluid was known. The temperature of the fluid at the inlet was set to 298K (ambient temperature of the air).
- A stationary wall boundary with no slip conditions was implied and a constant temperature for the bottom face of the channel was set to 323K.
- Reference values were set to fluid inlet conditions.
- Solution Methods: In pressure based solver the Pressure-Velocity coupling method was used, which derives the equation of pressure by the combination of continuity and momentum equations. Out of the four numerical algorithms

available in FLUENT, the SIMPLE (Semi-Implicit Method for Pressure-Linked Equations) method was used for simulations

- Governing equations: Fluent solver uses certain governing equations to solve flow problems. The primitive variable formulation expressed in terms of pressure and velocity as given below represents the three-dimensional Cartesian form of the continuity and momentum equations.

  The continuity equation (Conservation of mass): The density of the fluid remains constant as per assumption, the incompressible flow condition is invoked.

  $$\frac{\partial u}{\partial x}+\frac{\partial v}{\partial y}+\frac{\partial w}{\partial z}=0$$

  The momentum equation (Conservation of linear momentum - Newton's second law): The notations u, v, w represents the velocity components in the x, y and z directions respectively.

  $$\frac{\partial u}{\partial t}+\frac{\partial}{\partial x}\left(u^2+\frac{p}{\rho}\right)+\frac{\partial}{\partial y}(uv)+\frac{\partial}{\partial z}(uw)=\rho g_x+\mu\left(\frac{\partial^2 u}{\partial x^2}+\frac{\partial^2 u}{\partial y^2}+\frac{\partial^2 u}{\partial z^2}\right)$$

  $$\frac{\partial v}{\partial t}+\frac{\partial}{\partial x}(uv)+\frac{\partial}{\partial y}\left(v^2+\frac{p}{\rho}\right)+\frac{\partial}{\partial z}(vw)=\rho g_y+\mu\left(\frac{\partial^2 v}{\partial x^2}+\frac{\partial^2 v}{\partial y^2}+\frac{\partial^2 v}{\partial z^2}\right)$$

  $$\frac{\partial w}{\partial t}+\frac{\partial}{\partial x}(uw)+\frac{\partial}{\partial y}(vw)\frac{\partial}{\partial z}\left(w^2+\frac{p}{\rho}\right)+=\rho g_z+\mu\left(\frac{\partial^2 w}{\partial x^2}+\frac{\partial^2 w}{\partial y^2}+\frac{\partial^2 w}{\partial z^2}\right)$$

- Spatial Discretization to interpolate the cell center values to the faces of the control volume, set to second order upwind method, the least-square cell-based method used for Gradients and second-order method set for interpolating face pressure.

- Initialization: Solution variables need to be initialized prior to solution calculations in iterative methods as a realistic guess improves the stability of solution and accelerates convergence.

- One last step before calculating solution was to ‘Case Check’ for setup errors. In Fluent Case, Check is a utility that checks for compliance in Grid, Boundary Conditions, Material Properties and Solver settings.

- Convergence: In the iterative method, convergence is achieved when the solution does not change with subsequent iterations. Overall momentum, energy, etc. conservation equations should be balanced up to a specific tolerance. When the energy residuals decrease to the order of 10^{-6} (default resolution in Fluent) the solution converges for the Pressure-based solver.

CHAPTER 5

RESULTS AND DISCUSSION

Once the solution has converged, fluid flow and heat transfer characteristics of the fluid due to varying bifurcation angle (BA) and channel aspect ratio (AR) can be studied based on pressure drop, flow velocity and temperature variations in the flow region. As shown in Figure 5.1 it is evident that the bifurcation angle has very little effect on pressure drop and is least for 30° bifurcation angle.

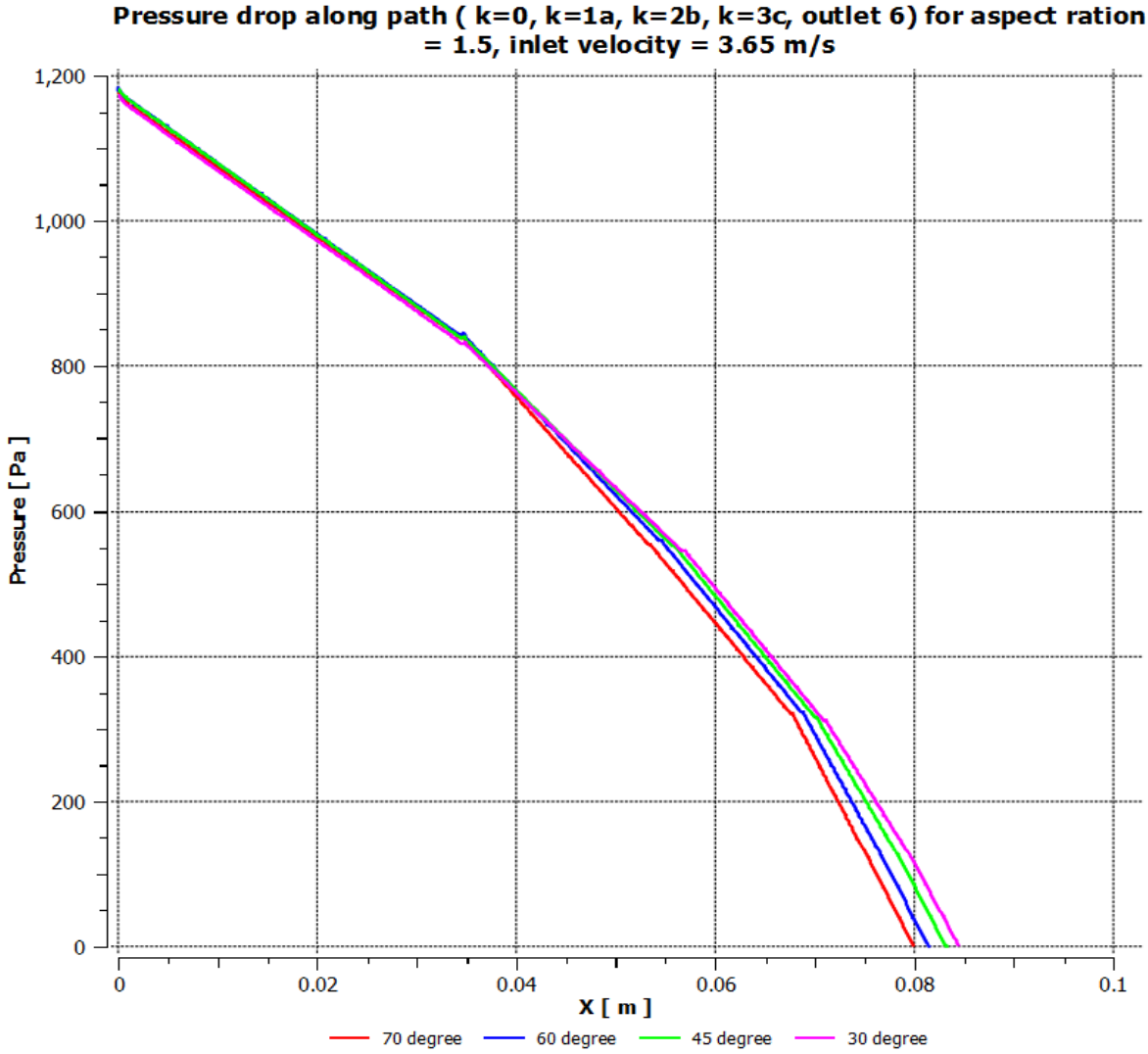

Figure 5.1. Pressure drop vs length for AR 1.5 and varying bifurcation angle

Though there is not much difference in pressure drop in the channels due to varying bifurcation angle, 30˚ angle delivers better performance due to uniformity in flow through each branch when compared to other bifurcation angles. The mass flow rate at outlets are as shown in Figure 5.2.

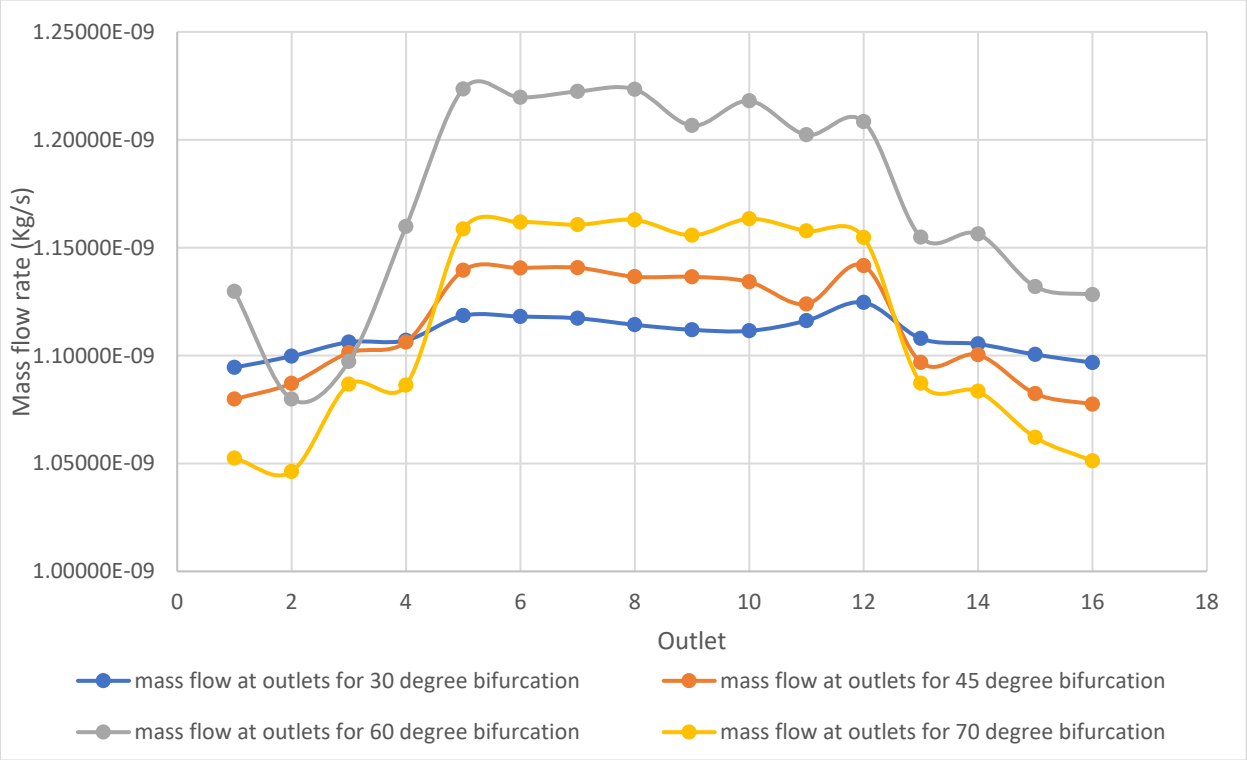

Figure 5.2. Mass flow rate vs outlet for varying bifurcation angle.

As the angle increases the uniformity in flow varies through outlets away from the center. For 60˚ angle, the variation is much higher than that of 70˚ angle.

Pressure drop against length of the channel for 30° bifurcation angle and varying aspect ratios of 0.5, 1.0, 1.5 and 2.0 are plotted as shown in Figure 5.3. Pressure drop is large for AR = 0.5 and reduces with increase in AR. Also, as the AR increases the difference in pressure drop and the channel length decreases.

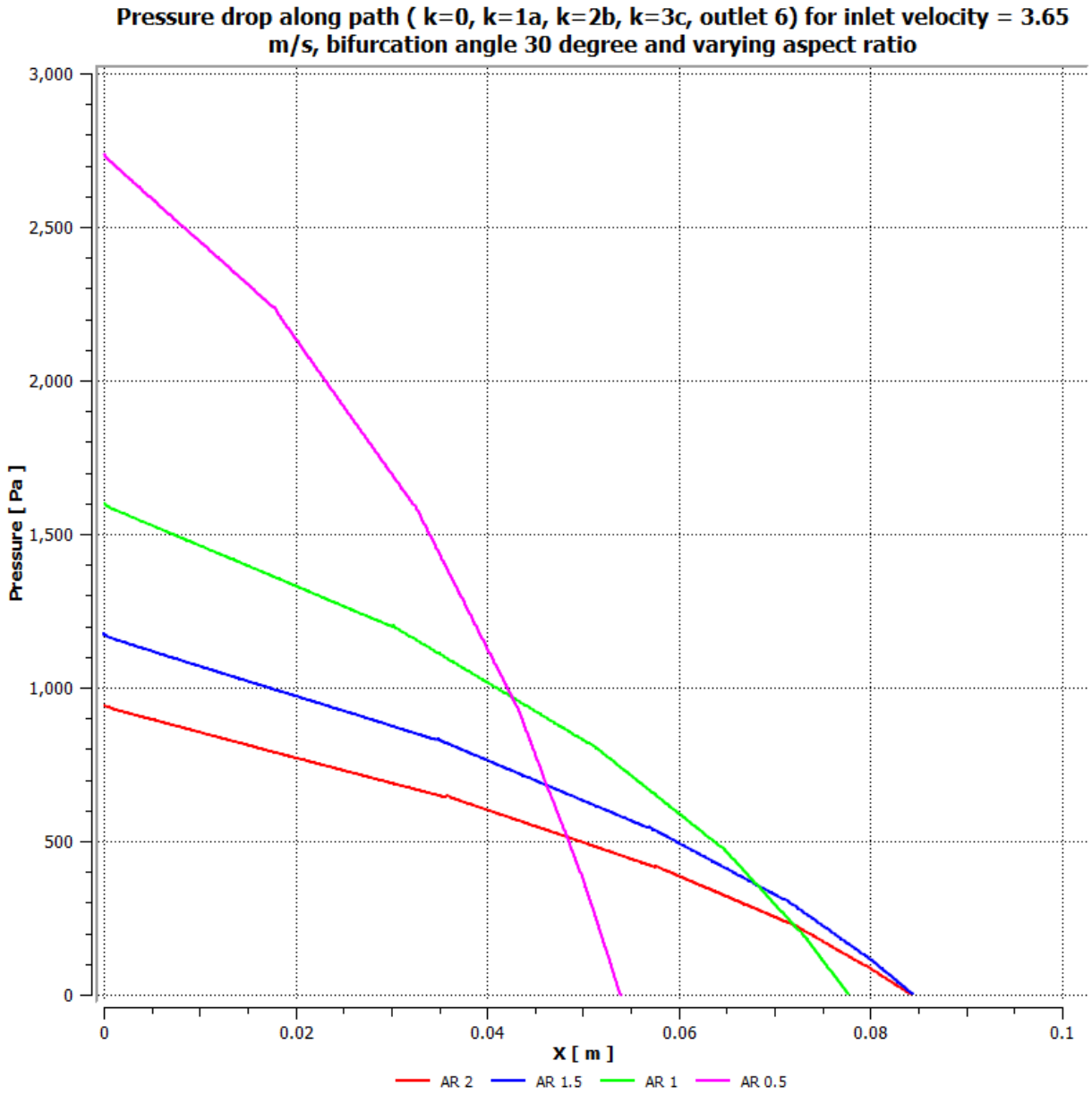

Figure 5.3. Pressure drop vs Length for 30° bifurcation angle and varying AR.

The cross-sectional area of the channels increases with each bifurcation due to the scaling method used in creating the geometry. Figure 5.4 shows a plot of channel cross-sectional area against branching level.

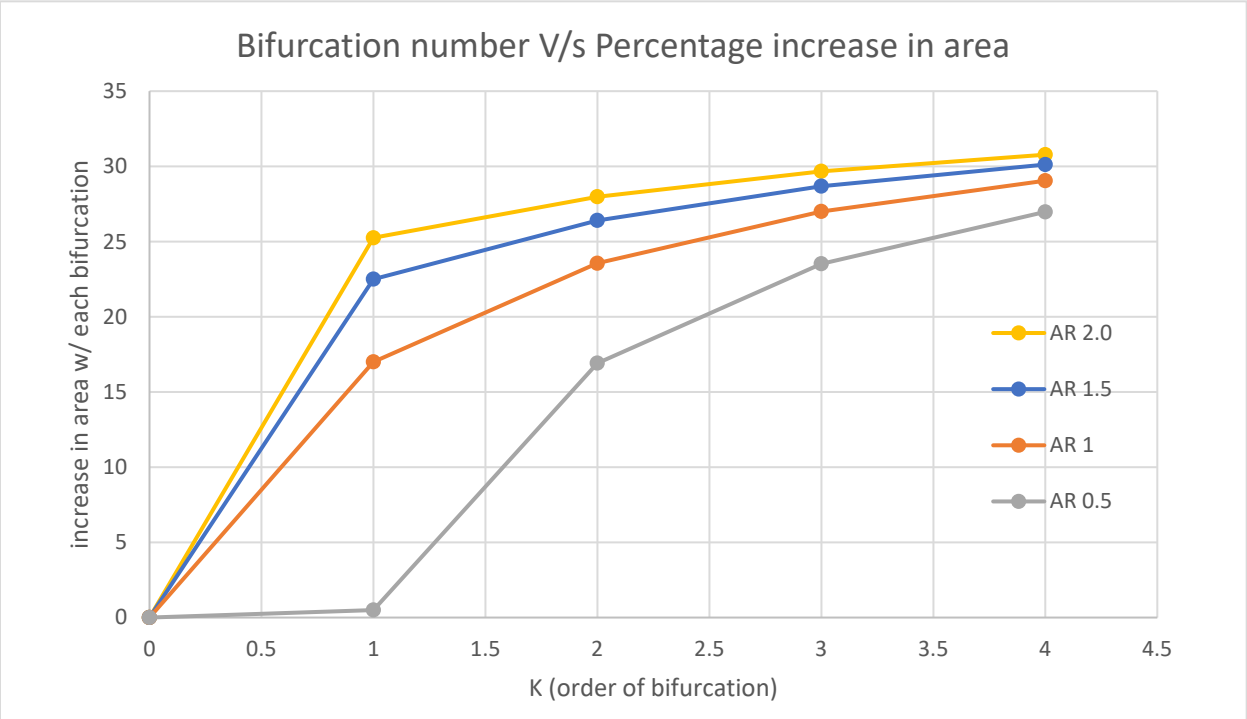

Figure 5.4. Increase in cross-sectional area vs bifurcation levels

Cross-sectional area after the first bifurcation for AR = 0.5 is negligible but shoots up by 17% at the second bifurcation, whereas there is a steady rise in area for increasing AR. The reason for the trend in pressure drop witnessed in the previous section can be attributed to the relation observed with increasing cross-sectional area due to the bifurcation.

Pressure difference due to change in inlet velocity. Velocity value of 3.05m/s as calculated from channel dimension and volume flow rate for AR 2.0, 3.65m/s value as calculated for AR 1.5. As seen from the plot the pressure drop is greater for higher velocity value for the same geometry and conditions.

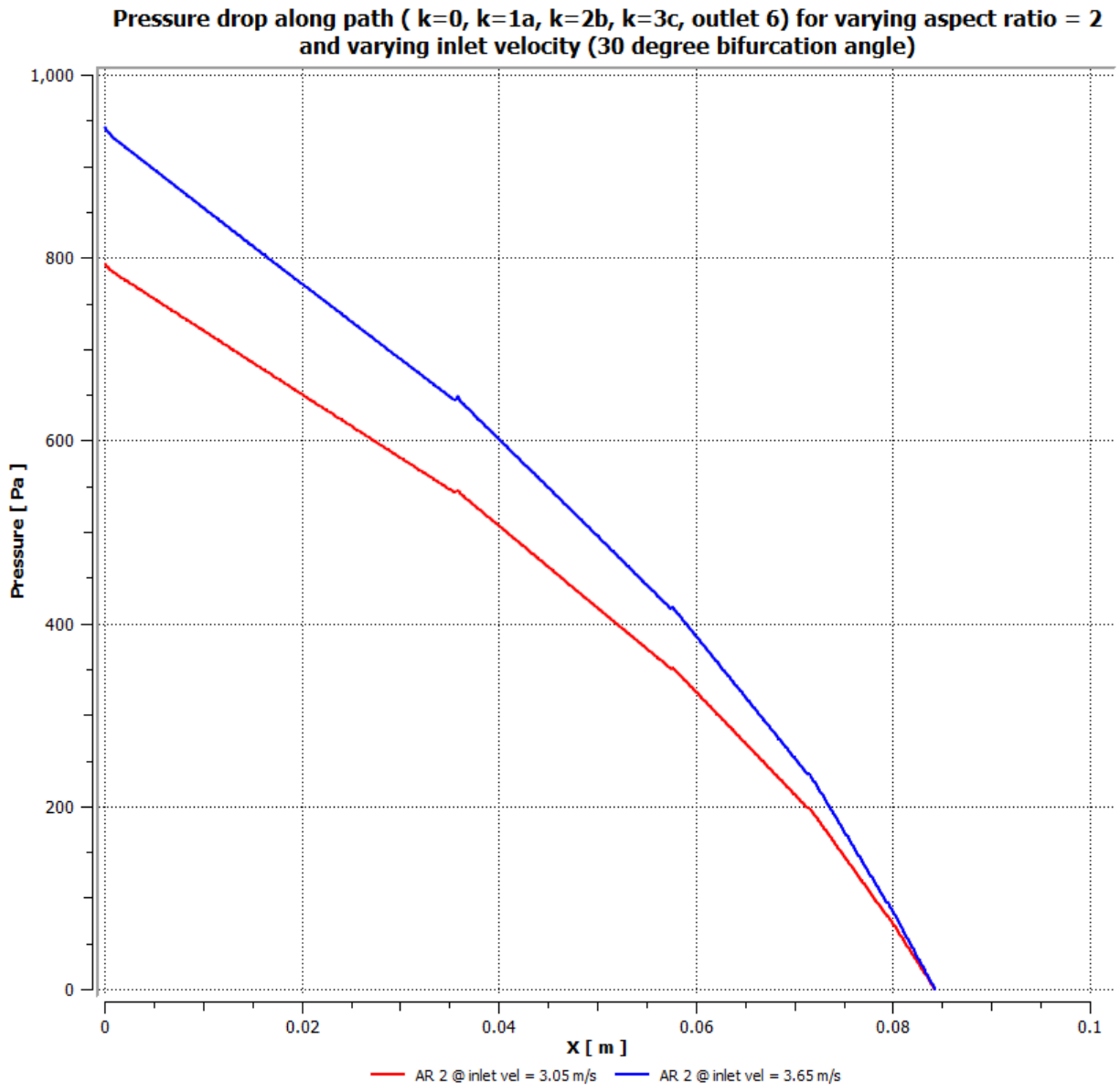

Figure 5.5. Pressure drop vs length for varying inlet velocity

Pressure drop values for different inlet velocity plotted earlier showed an increase in pressure drop due to increase in velocity. By plotting non-dimensional quantities P/Pmax vs x/L, it is evident that the trend in pressure drop is the same as the plots coincide with each other.

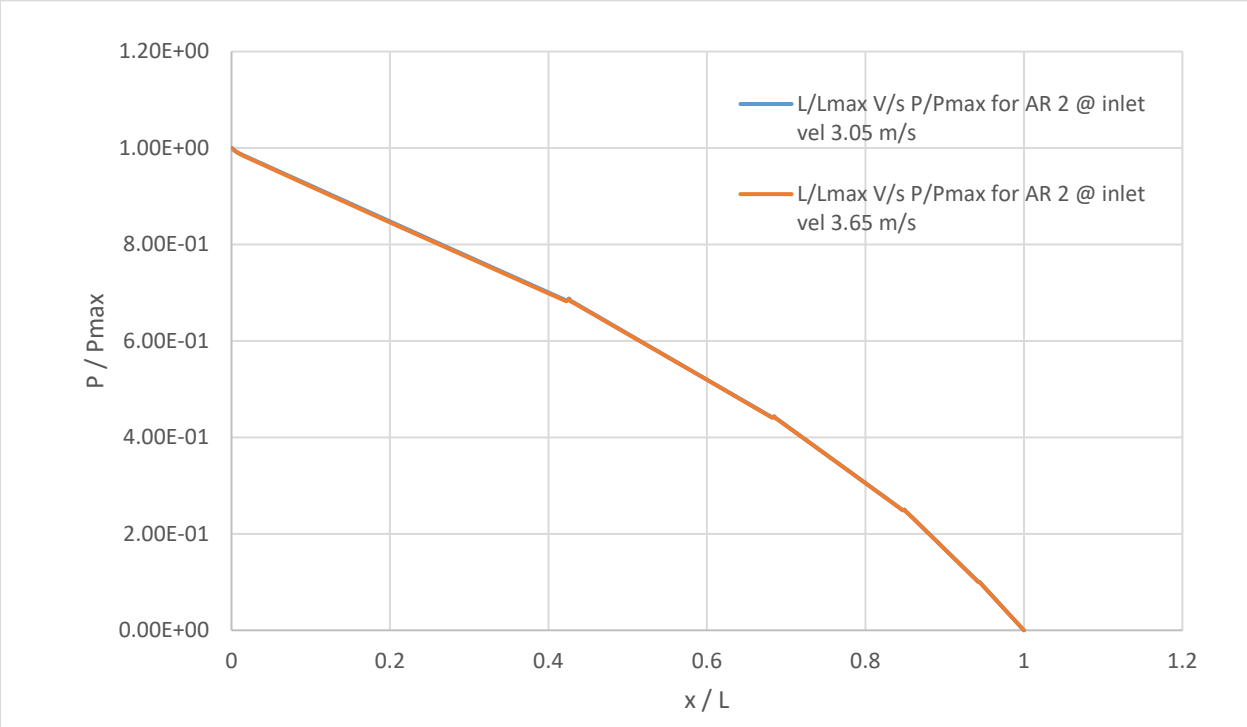

Figure 5.6. Pressure drop analysis through non-dimensional entities for varying inlet velocity

Effect of number of bifurcations is one of the difficult results to compare. The pressure drop due to zero, one, two, three and four bifurcations were simulated. Palpably pressure drop increases with each bifurcation. With the help of dimensionless quantities, the pressure drop with respect to the length of the channel as plotted in Figure 5.7. Visibly a spike in pressure value occurs at the bifurcation. Therefore, with each bifurcation, an increase in pressure leads to decrease in total pressure drop through the channels.

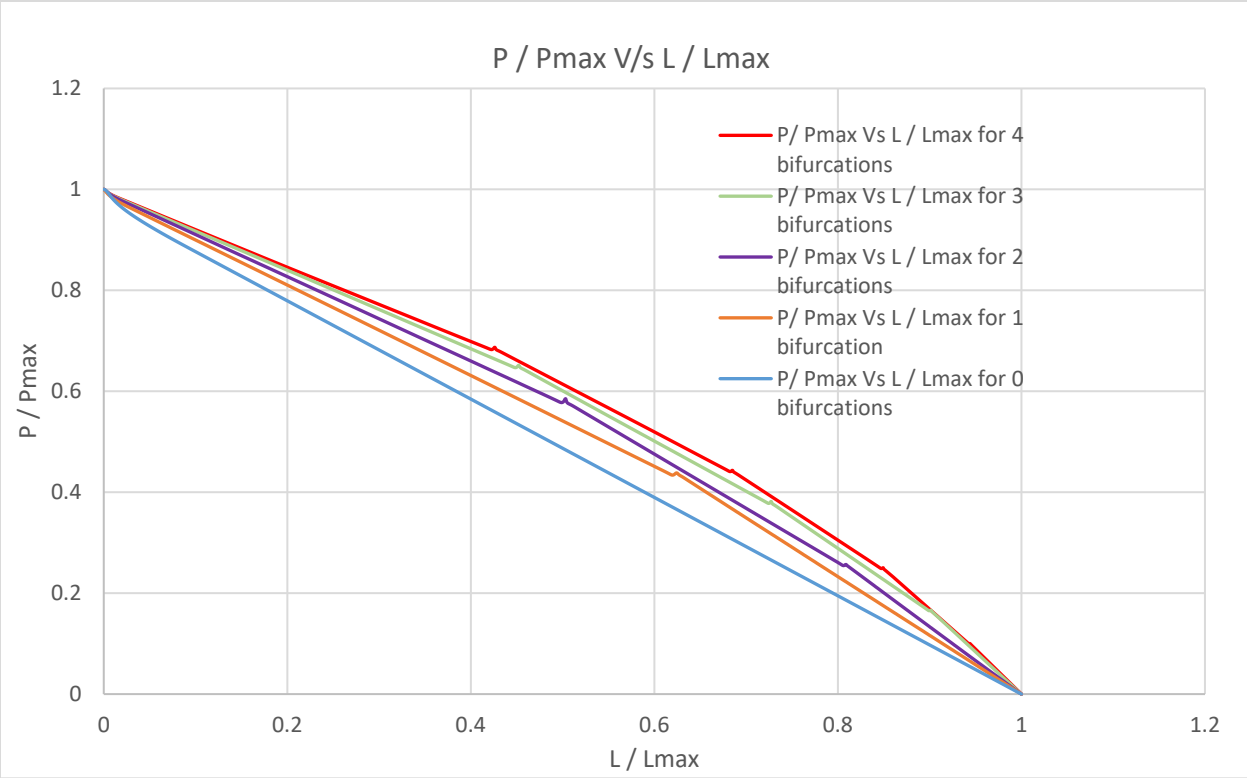

Figure 5.7. Normalized Pressure vs length for 30˚ bifurcation angle and AR = 2.0.

The temperature profile is drawn along the velocity streamline running through the above-mentioned flow path. The temperature profile of 30, 45and 70-degree bifurcation angle are coincidental whereas 60-degree has a slight deviation. Velocity streamline is generated by the software and may not follow the same path for all cases. Hence, the deviation of temperature profile in Figure 5.8.

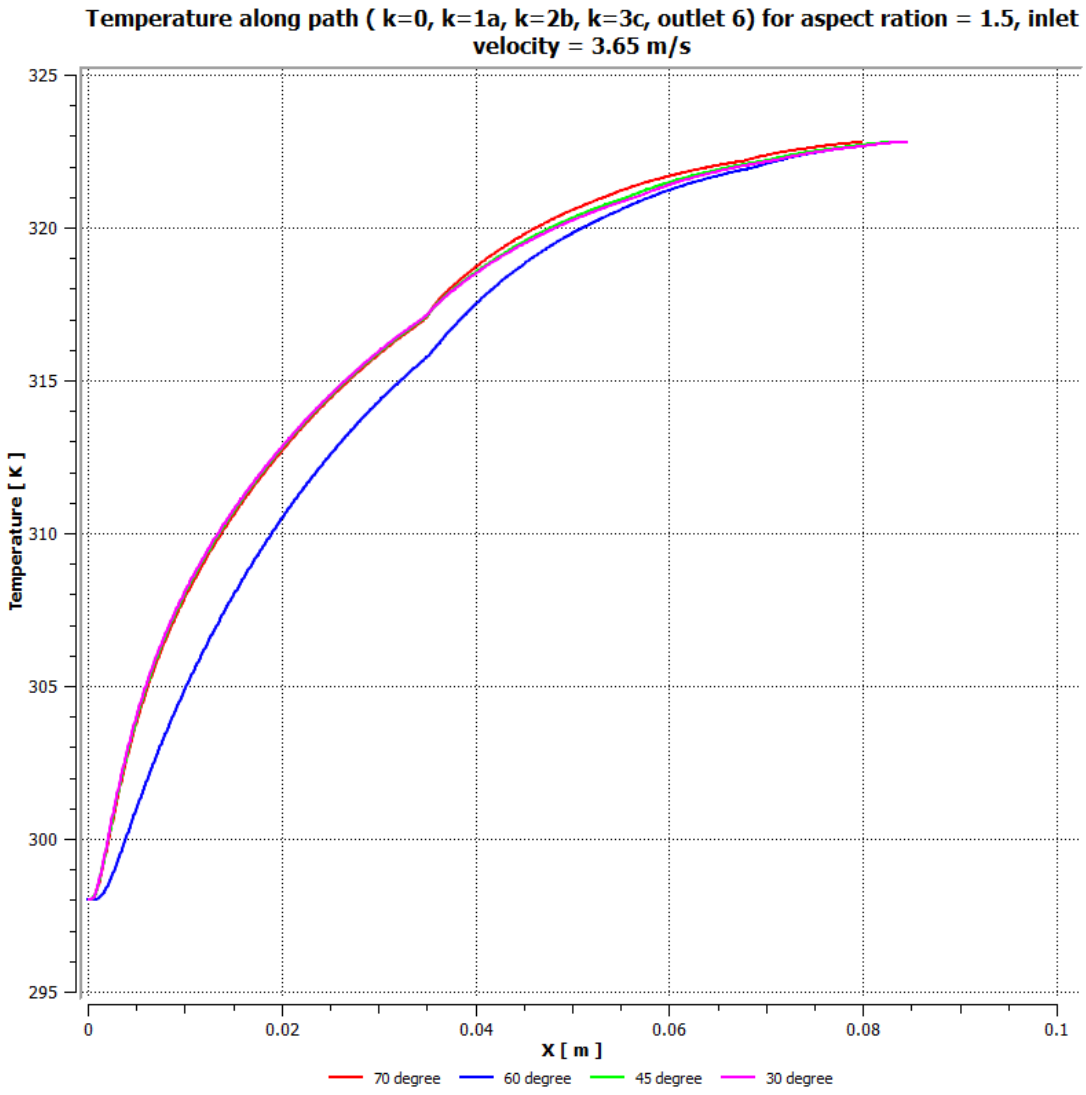

Figure 5.8. Temperature vs Channel length for AR = 1.5 and varying bifurcation angle.

The temperature profile of the fluid flow along the velocity streamline through the mentioned path of the flow clearly indicates that increase in AR leads to increase in surface area of channel. And also the heated surface area reduces compared to the total surface area of the channel. Therefore the rise in air (working fluid) temperature is slower in comparison with lower ARs. Better uniformity in the temperature of the air through the channel is achieved.

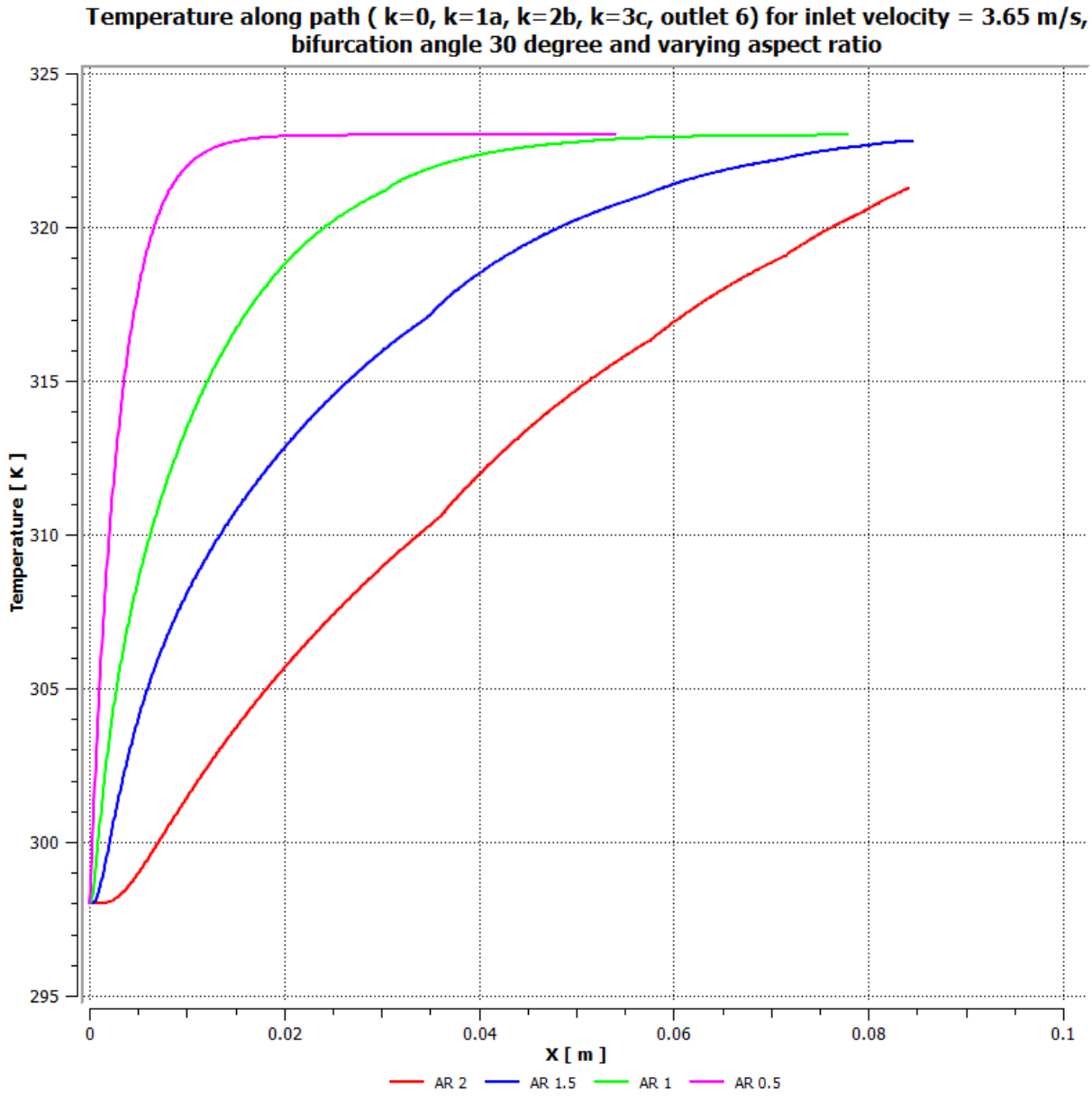

Figure 5.9. Temperature vs Channel length for 30˚ bifurcation angle and varying AR.

Length of the channel, and in turn the total surface area increases with each bifurcation. As discussed in the previous section, a slight increase in pressure drop at bifurcations lowered the total pressure drop across the channel length. Non-dimensional entities are used to compare the effect of number of bifurcations on variations in temperature across the channel length. As shown in Figure 5.10 the non-dimensional temperature profile shows the rate at which temperature rises, slows down with each bifurcation.

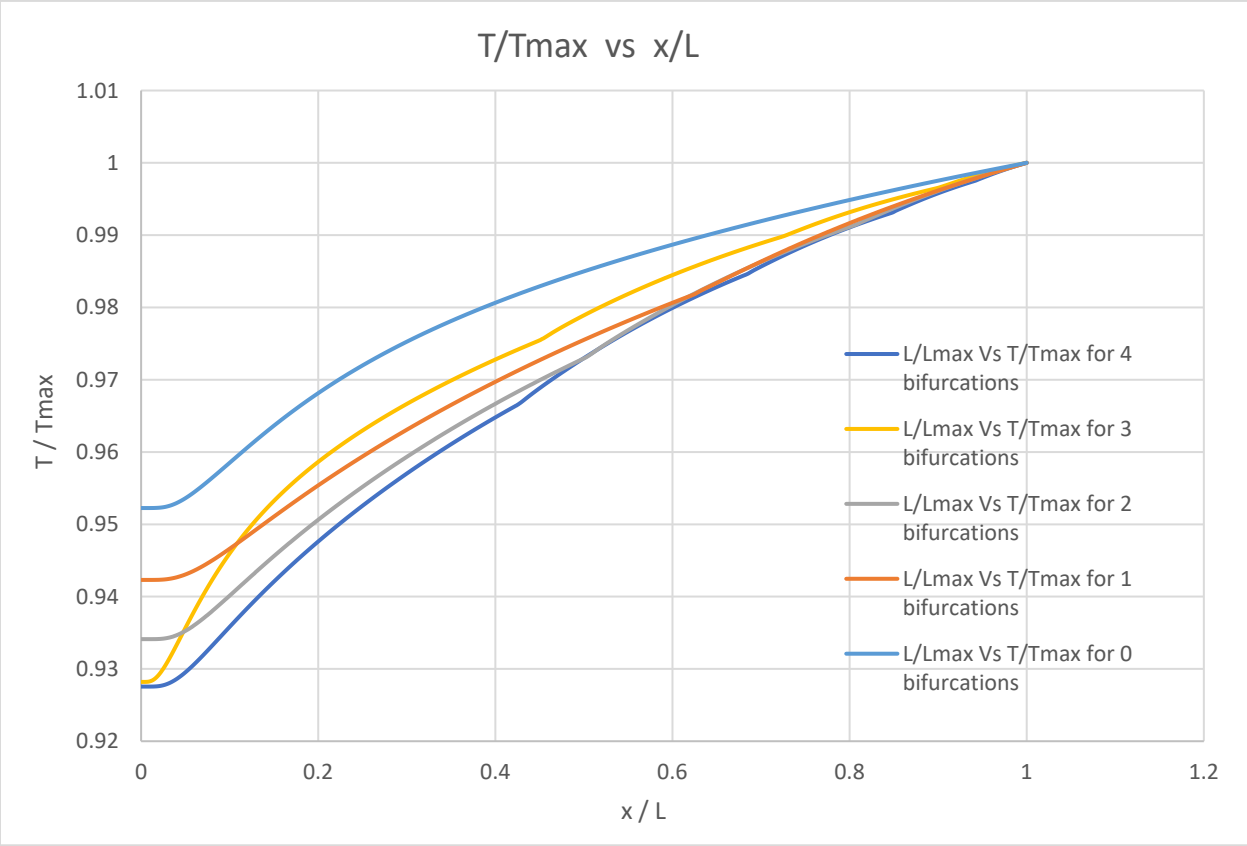

Figure 5.10. Non-dimensional temperature profile for 30˚ bifurcation angle and AR = 2.0.

So far, the simulations and results were discussed for the constant wall temperature at the bottom face of 323K. The effect of different temperatures at the bottom face of the channel as shown in Figure 5.11 illustrates that even with a temperature difference of 225K between the fluid and wall, the fluid temperature gets close to wall temperature only in the fourth bifurcation.

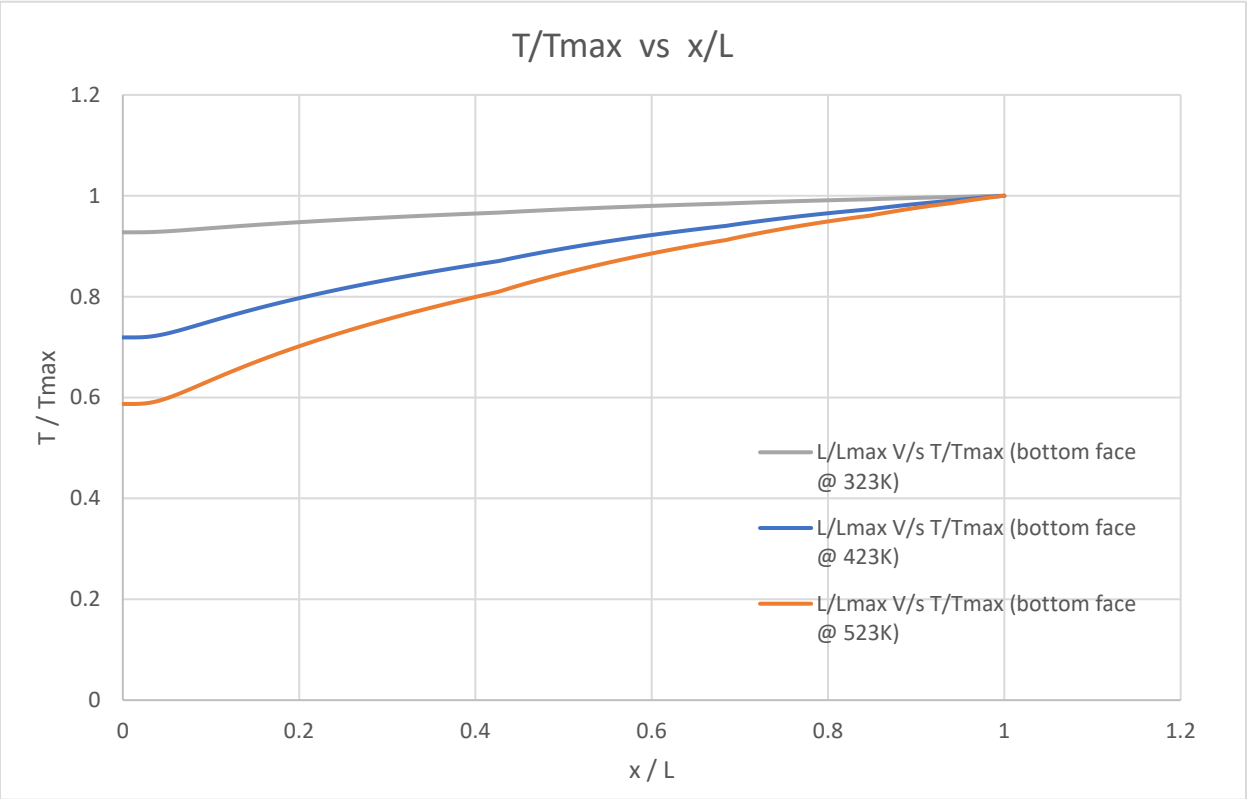

Figure 5.11. Non-dimensional temperature profile for AR = 2 at inlet

5.1 Conclusion

Bifurcation angle and channel aspect ratio were the two important variables in this study. The fluid flow and heat transfer characteristics were evaluated through pressure drop and temperature profiles through the length of the channel.

The difference in value of Pressure drop observed due to varying bifurcation angle was insignificant but, the values of mass flow rates at different outlets displayed uniformity in flow for 30˚ branching angle. Pressure drop values decreased by a large value with increase in AR. Pressure drop for AR 2.0 was noticed to be less than 2.5 times the value obtained for channel AR 0.5.

Although temperature profiles for varying bifurcation angles again showed no significant difference, the variations due to change in AR were sound and clear that for higher AR the maximum temperature attained by the fluid is less than the wall temperature. This observation is attributed to decreasing ratio of heated wall surface area to that of total surface area of the channels. It varies from $1/3^{rd}$ for AR = 0.5 to $1/6^{th}$ for AR = 2.0.

Therefore, a conclusion can be drawn based on the current study that, for the considered geometrical parameters a 30˚ bifurcation angle and an aspect ratio of 2.0 induces uniform flow and heat transfer through branched structure microchannels.

5.2 Future Recommendations

The research so far in the fractal or tree-like branching channel networks were all carried out computationally. The main reason behind it is due to unavailability of technology to produce such complex designs at the microscale level. With improvements in the field of 3-D printing, in the near future, it is possible to 3-D print metals in complex shapes and sizes which in turn can lead to experimental validation of the numerical studies carried out so far.

Regarding working fluid, depending on the application different fluid with varying viscosity, density, thermal conductivity, etc., can be analyzed. One of the best application for branching channel would be in blood transfusion to maintain uniform blood temperature.

In applications related to cryogenics or any other multi-phase fluid when used in the cooling process, the pressure variations can be unpredictable and cannot be solved by the analytical method. In which case, a computational solution to such problems can provide insight on how the geometrical and boundary conditions affect the flow and heat transfer properties of the fluid.

REFERENCES

REFERENCES

1. D. B. Tuckerman and R. F. W. Pease., "High-Performance Heat Sinking for VLSI," *IEEE Electron Device Lett*., Vol. EDL-2, 1981, pp. 126–129.

2. Obot, N. T., "Towards a Better understanding of Friction and Heat/Mass Transfer in Microchannels – A Literature Review," *Proc. International Conference on Heat Transfer and Transport Phenomena in Microscale*, Banff, Canada, Begell House, New York, pp. 72-79.

3. D. Keith Walters et al., "A Method for Three-Dimensional Navier-Stokes Simulations of Large-Scale Regions of the Human Lung Airway," *Journal of Fluids Engineering – ASME*, Vol. 132, 2010.

4. Weibel, E. R., Morphometry of the Human Lung, *Academia*, New York, 1963.

5. Pence, D. V., "Improved Thermal Efficiency and Temperature Uniformity Using Fractal-Like Branching Channel Networks," *Proc. International Conference on Heat Transfer and Transport Phenomena in Microscale*, Banff, Canada, Begell House, New York, 2000, pp. 142-148.

6. Pence, D. V., "Reduced Pumping Power and Wall Temperature in Microchannel Heat Sinks with Fractal-Like Branching Channel Networks," *Microscale Thermophys. Eng.*, 6(4), 2002, pp. 319-330.

7. West, G. B., et al., "A General Model for the Origin of Allometric Scaling Laws in Biology," *Science*, 276, 1997, pp. 122-126.

8. Ali, Y. Alharbi., "Fluid Flow through Microscale Fractal-Like Branching Channel Networks," *Journal of Fluids Engineering - ASME*, Vol. 125(6), 2004, pp. 1051-1057.

9. Ali, Y. Alharbi., "Thermal Characteristics of Microscale Fractal-Like Branching Channels" *Journal of Heat Transfer, ASME*, Vol. 126(5), 2004, pp. 744-752.

10. Wang et al., Effect of Bifurcation Angle in Tree-Shaped Microchannel Networks" *Journal of Applied Physics*, Vol. 102, 2007.

11. Yongping Chen., and Ping Cheng., "Heat Transfer and Pressure Drop in Fractal Tree-Like Microchannel Nets," *International Journal of Heat and Mass Transfer*, Vol. 45, 2002, pp. 2643-2648.

12. Sobhan, B., and Garimella, S. V., "A Comparative Analysis of Studies on Heat Transfer and Fluid Flow in Microchannels, *Microscale Thermophys. Eng*., Vol. 5, 2010, pp. 293-311.

13. Wu, Peiyi, and W. A. Little. “Measurement of the heat transfer characteristics of gas flow in fine channel heat exchangers used for microminiature refrigerators.” *Cryogenics*, Vol. 24, No. 8, 1984, pp. 415-420.

14. Kandlikar, Satish G., Stéphane Colin, Yoav Peles, Srinivas Garimella, R. Fabian Pease, Juergen J. Brandner, and David B. Tuckerman. “Heat transfer in microchannels—2012 status and research needs.” *Journal of Heat Transfer,* Vol. 135, No. 9, 2013, 091001.

15. Galvis, E., S. Yarusevych, and J. R. Culham., “Incompressible laminar developing flow in microchannels,” *Journal of Fluids Engineering*, Vol. 134, No. 1 2012, 014503.

16. Garimella, Suresh V., and Choondal B. Sobhan, “Transport in microchannels - A critical review,” *Annual review of heat transfer*, Vol. 13, No. 13, 2003.

17. Horsfield, Keith, and Gordon Cumming, “Morphology of the bronchial tree in man,” *Journal of Applied Physiology,* Vol. 24.3, 1968, pp. 373-383.

18. Douglas Benjamin Heymann, “On the Optimization of Performance in Fractal-like Branching Microchannel Heat Transfer Devices,” Thesis Dissertation Report, 2010.

19. Chen Lingen, Huijun Feng, Zhihui Xie, and Fengrui Sun, “Thermal efficiency maximization for H-and X-shaped heat exchangers based on constructal theory.” *Applied Thermal Engineering,* Vol, 91, 2015, pp. 456-462.

20. Kitaoka, Hiroko, Ryuji Takaki, and Béla Suki., “A three-dimensional model of the human airway tree.” *Journal of Applied Physiology*, Vol. 87.6, 1999, pp. 2207-2217.

21. Hammersley, JEFFREY R., and D. E. Olson, “Physical models of the smaller pulmonary airways.,” *Journal of Applied Physiology*, Vol. 72.6, 1992, pp. 2402-2414.

22. Sahar, Amirah M., Jan Wissink, Mohamed M. Mahmoud, Tassos G. Karayiannis, and Mohamad S. Ashrul Ishak, “Effect of hydraulic diameter and aspect ratio on single phase flow and heat transfer in a rectangular microchannel.” *Applied Thermal Engineering*, 115, 2017, pp. 793-814.

23. Gerken, Iris, Juergen J. Brandner, and Roland Dittmeyer, “Heat transfer enhancement with gas-to-gas micro heat exchangers.” *Applied Thermal Engineering*, Vol. 93, 2016, pp. 1410-1416.

24. Fan, Yilin, and Lingai Luo., “Recent applications of advances in microchannel heat exchangers and multi-scale design optimization.” *Heat Transfer Engineering,* Vol. 29, No 5, 2008, pp.461-474.

25. Haber, Shimon, Alys Clark, and Merryn Tawhai., “Blood flow in capillaries of the human lung.” *Journal of biomechanical engineering*, Vol. 135, No. 10, 2013, 101006.

26. Wechsatol, W., S. Lorente, and A. Bejan., "Optimal tree-shaped networks for fluid flow in a disc-shaped body." *International Journal of Heat and Mass Transfer,* Vol. 45, No. 25, 2002, pp. 4911-4924.

27. Lee, Poh-Seng, and Suresh V. Garimella., "Thermally developing flow and heat transfer in rectangular microchannels of different aspect ratios," *international journal of heat and mass transfer,* Vol. 49, No. 17, 2006, pp. 3060-3067.

28. Fox, Robert W., Alan T. McDonald, and Philip J. Pritchard., "*Introduction to fluid mechanics*," New York: John Wiley & Sons, Vol. 5, 1998.

29. POPESCU Traian, Mircea MARINESCU, Horaţiu POP3 Gheorghe POPESCU and Michel FEIDT., "MICROCHANNEL HEAT EXCHANGERS–PRESENT AND PERSPECTIVES," *UPB Sci Bull Ser D,* Vol. 74 2012, pp. 55-70.

30. Kandlikar, Satish G., "Heat transfer mechanisms during flow boiling in microchannels," *Transactions-American Society of Mechanical Engineers Journal of Heat Transfer,* Vol. 126, No. 1, 2004, pp. 8-16.

31. Bejan, Adrian, "Shape and structure, from engineering to nature," *Cambridge university press,* 2000.

32. Kandlikar, Satish G., "History, advances, and challenges in liquid flow and flow boiling heat transfer in microchannels: a critical review," *Journal of heat transfer,* Vol. 134, No. 3, 2012, 034001.

33. Colin, Stéphane., "Gas microflows in the slip flow regime: a critical review on convective heat transfer," *Journal of Heat Transfer,* Vol. 134, No. 2, 2012, 020908.

34. Kandlikar, Satish G., and William J. Grande., "Evaluation of single-phase flow in microchannels for high heat flux chip cooling—thermohydraulic performance enhancement and fabrication technology.," *Heat transfer engineering,* Vol. 25, No. 8, 2004, pp. 5-16.

35. Steinke, Mark E., and Satish G. Kandlikar, "Single-phase heat transfer enhancement techniques in microchannel and minichannel flows," *International Conference on Microchannels and Minichannels, Rochester, NY,* 2004, pp. 17-19.

36. Kakaç, Sadik, Hafit Yüncü, and Kunio Hijikata, eds, "Cooling of electronic systems, *Springer Science & Business Media,* Vol. 258, 2012.

37. Bejan, Adrian, "Constructal-theory network of conducting paths for cooling a heat generating volume," *International Journal of Heat and Mass Transfer,* Vol. 40, No. 4, 1997, pp. 799813-811816.

38. ANSYS Fluent Theory Guide version 16.2